SURGICAL ROBOTICS

Montpellier, France

Pôle Universitaire Européen de Montpellier et du Languedoc-Roussillon

LIRMM Laboratoire d'Informatique de Robotique et de Microélectronique de Montpellier

Frontiers of Endoluminal Robotics Surgery (Part 2)

Cesare Stefanini

Scuola Superiore Sant'Anna
Pisa, Italy

CRIM a lab of inventors and entrepreneurs

Evolution of surgical robotics

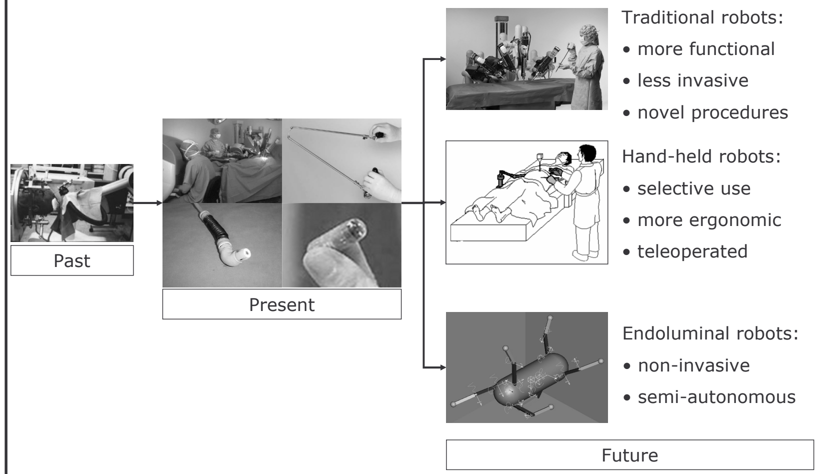

Evolution of surgical robotics

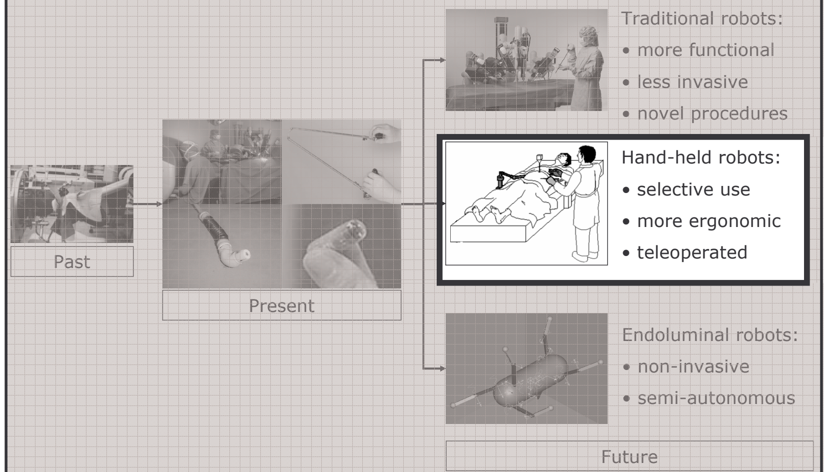

Extending the surgeon's arm

- A simpler robot assistant
- "Close teleoperation" concept:
  - *One hand* controls a laparoscopic instrument
  - *The other hand* acts as HMI for a surgical robot

Research performed in the context of the ApprEndo FIRB/MIUR Project (TIE 2001 Programme)

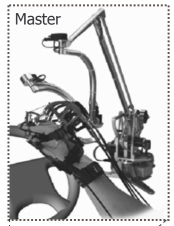

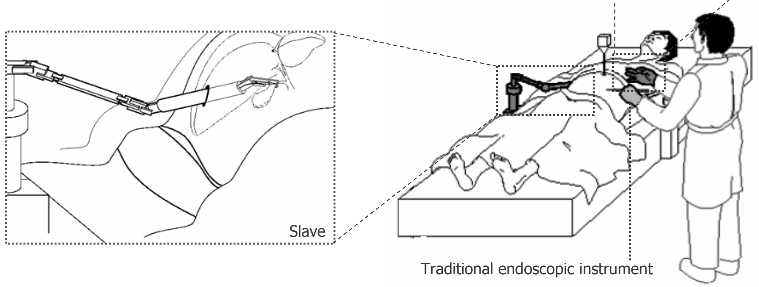

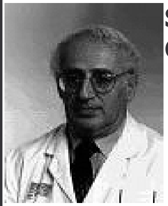

Sir Alfred Cuschieri, MD

The operating room of the year 2030 will be a totally different environment than today

MASS Screening and EARLY diagnosis will have a major impact on the type and invasiveness of required surgical procedures

The combination of micro/nano tecnologies and microrobotics will enable to perform active monitoring and diagnostics in advanced and early manners, and will be also one of the key technologies enabling future high quality, early and minimal invasive surgery

NeuroEndoscopy of the spinal cord: **the Problem**

There is need for:

- Precise and early diagnosis of spinal cord lesions (300.000 paralyzed persons in Europe)
- Possibility to intervene directly on pathologies:
  - Injection of neurotransmitters and pumping of haematomas in **traumatic lesions**
  - Cleaning of fibrous adherences in case of **arachnoid proliferation**
  - electro-coagulation of the afferences to the posterior horn in case of **intractable pain**

BUT:

Current procedures are limited to the **epidural space**, **far** from the spinal cord and filled by semiliquid, **not transparent** fat.

Therefore:

Need for an Endoscopic System for the **navigation** inside the **subarachnoid space** (filled by the Cerebro Spinal Fluid), for diagnosis and intervention.

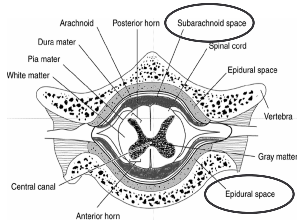

Current spinal endoscopy: epiduroscopy

Severe, chronic back pain can persist after multiple types of treatment, and possibly even after back surgery. With epiduroscopy the doctor makes a small incision (less than 10 mm long) in the lumbar part, near to the tail bone. A catheter is inserted through a needle into the epidural space and medication is injected. A fiberoptic scope is inserted through the catheter to detect the presence of scar tissue.

Spinal Endoscopy dates back to 1931 with the publication of the work of Berman. During the experiment, the nervous tissue and blood vessels were seen coursing over the lumbar spine, although not very clearly. Any practical application would have to wait on the development of improved visualization systems.

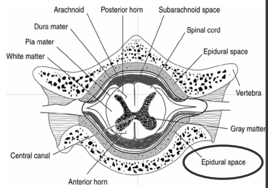

Epiduroscopy however is still limited to the epidural space and can only enable back pain treatment.

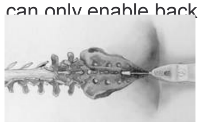

Neuroendoscopy of Spinal Cord: the environment

- The sub-arachnoid space is comprised between two meninxes, **dura mater and pia mater,** immediately below a third meninx called **arachnoid.**
- It is crossed by anatomical structures
  - **Blood vessels**
  - **Nerve roots**
- Endoscopic techniques for the exploration of the spinal cord would provide us with
  - Direct vision of the region of interest
  - MRI and TC are not usually helpful
  - Possibility of making biopsy, injection of neurotransmitters, pumping of haematomas, cleaning of fibrous adherences, in a non-invasive way

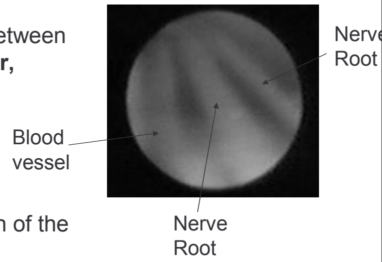

Neuroendoscopy of Spinal Cord: the environment

- The mean is very indicate for navigation (**Cerebro-Spinal Fluid, water-like liquid**)

- CSF is transparent.
- CSF is secreted continuously (**0.35 ml/minute**) and replaced completely every 6 to 8 hrs.
- Since CSF is basically a plasma filtrate with very few cells, it can be replaced by an artificial fluid (using NaCl, KCl, $CaCl_2 \cdot 2H_2O$, $MgCl_2 \cdot 6H_2O$, $Na_2HPO_4 \cdot 7H_2O$, $NaH_2PO_4 \cdot H_2O$ and water).
- During the procedure, the artificial CSF can be used to keep the concentration, pressure and volume of the fluid within the space nearly constant.

Neuroendoscopy of Spinal Cord: the environment

- The mean is very indicate for navigation (Cerebro-Spinal Fluid, water-like liquid)
- The **workspace is extremely small**

Size of the Sub Arachnoid Space, mm

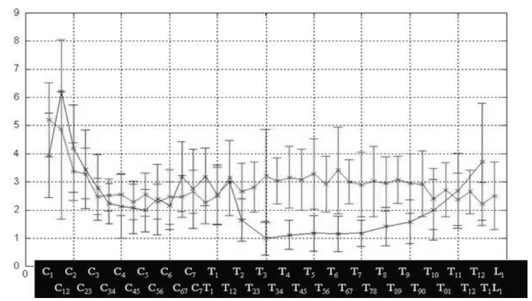

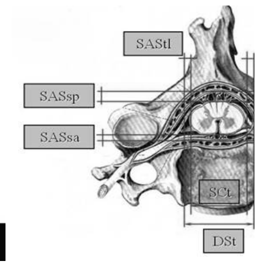

Neuroendoscopy of Spinal Cord: the environment

- The mean is very indicate for navigation (Cerebro-Spinal Fluid, water-like liquid)
- The workspace is extremely small
- Anatomical **structures are very DELICATE** (vessels, nerve roots)

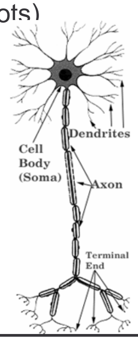

AXONAL DAMAGE

For cord tissue, shear **strains** under 5% represent no injury, 5 - 10% represent mild injury, 10 - 15% represent moderate injury and strains above 15% represent severe injury.

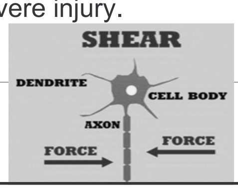

An advanced concept for Robotic Neuroendoscopy

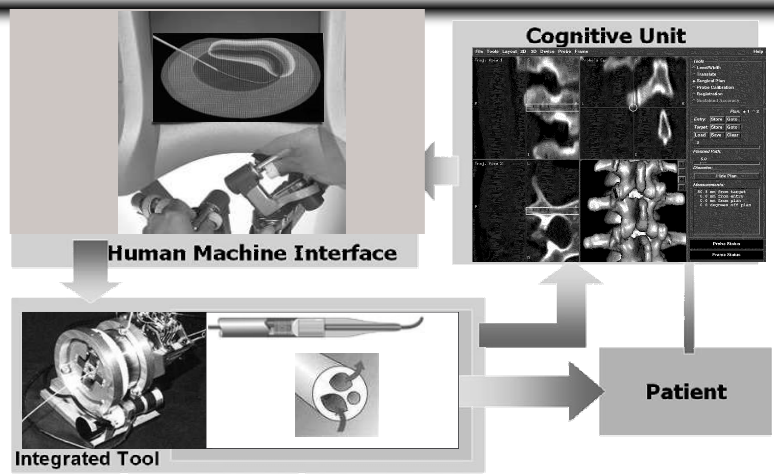

The Minosc solution - architecture

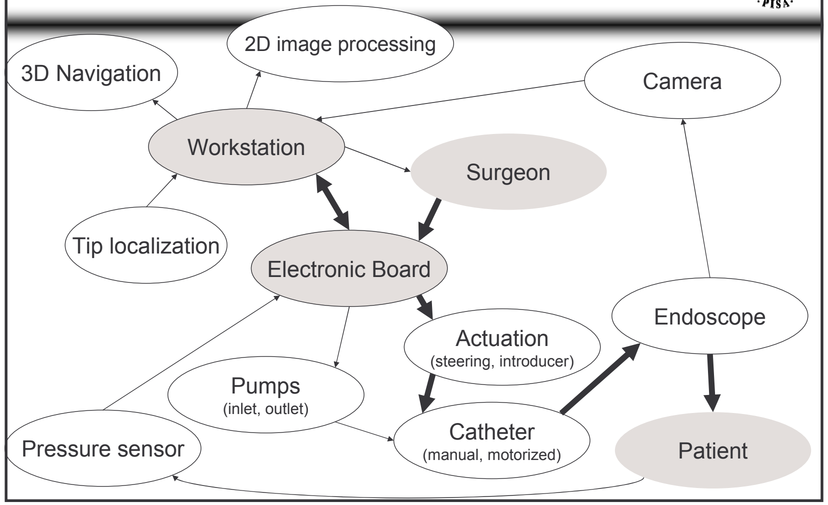

The catheter as a dexter **carrier** of tools

- ***View***: *Endoscope*
- ***Ablation***:
  - *Laser*
  - *Rotating Blades/mills*
- ***Diagnosis***:
  - *Ultrasound*
- ***Local drug delivery***
- ***Micromanipulation and Micropositioning*** *of bioartificial substitutes*

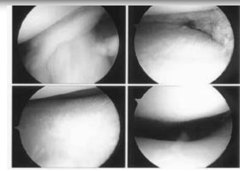

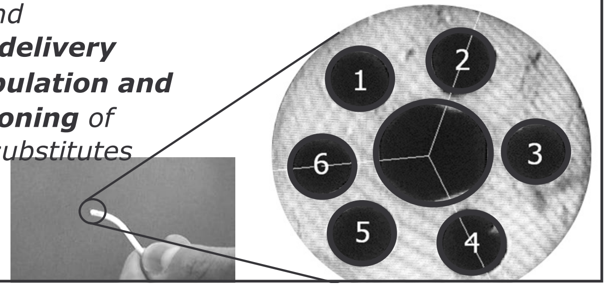

The working modalities

Manual	The surgeon has complete control on the tip: the system signals dangerous situations (imminent collisions,…)
Semi-automatic	***The surgeon has the control on the steering system, but the navigation module doesn't allow him to navigate too close to delicate structures***
Automatic	The control of the intruder and of the steering system is left to the navigation module, programmed to reach a "target".

MINOSC – The **Actuated Catheter**

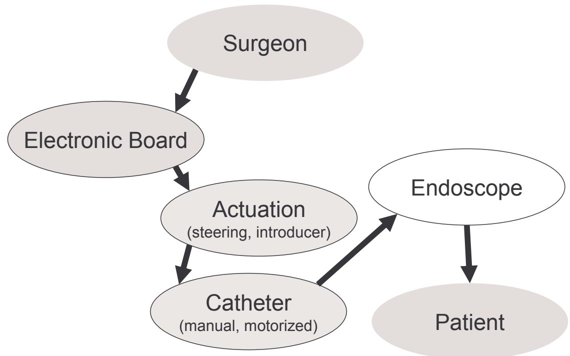

MINOSC – The **Actuated Catheter**

The concept:

- **Mechanical Steering** of the endoscope using *flexure joints* fabricated via Graded Material Technology and Injection Molding.

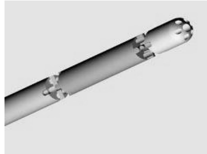

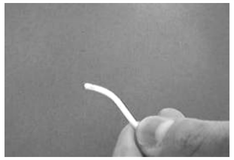

- **Servoassisted introducer** for fine and controlled advancement of the endoscope. Servomotor actuating a STORZ micromanipulator.

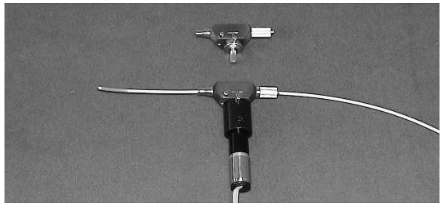

MINOSC – The **Actuated Catheter**

The first prototype which has been fabricated is a manually steerable system for standalone, hand-held use.
Two degrees of freedom, cable driven through a 4 cable joystick

Micro endoscope:

6000 Pixels
0.5 mm diam. (illumination included)
Autoclavable

(Karl Storz)

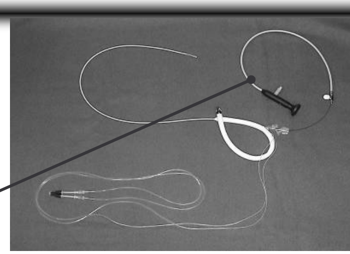

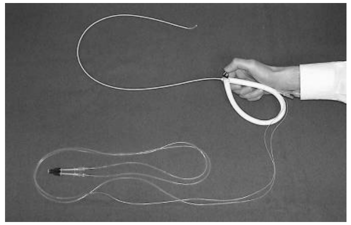

MINOSC – The **Actuated Catheter**

The second prototype which has been fabricated is a servoassisted system using two stepper motors. Two degrees of freedom, cable driven through a **3** cables system, maintaining the sum of the three lengths constant.

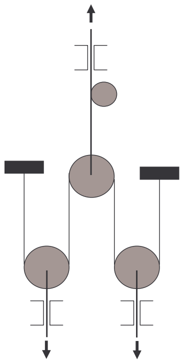

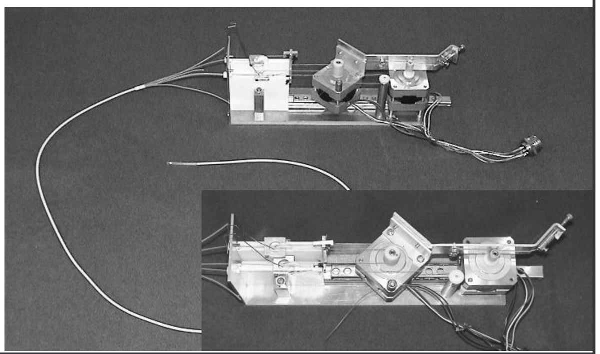

MINOSC – The **Actuated Catheter**

Equations for the cable

$$\begin{cases} \underline{\Delta F} = \underline{\tau}(\underline{R} - d)\underline{\Delta\alpha} \\ F = \underline{p}(R - d) \end{cases}$$

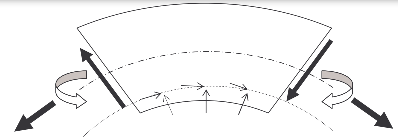

Equations for the catheter

$$\begin{cases} -\underline{\Delta N} - T\Delta\alpha + \tau\Delta\alpha(R-d) = 0 \\ N\Delta\alpha - \underline{\Delta T} - p\Delta\alpha(R-d) = 0 \\ -\underline{\Delta M} + R\Delta N - (R-d)^2\tau\Delta\alpha = 0 \end{cases}$$

Tangential friction:

$$\tau = p\mu + \tau_0$$

Catheter elasticity

$$\begin{cases} 1/R = M/EJ \\ \underline{\varepsilon} = N/EA \\ \Delta L = \Delta L_0(1+\varepsilon) \end{cases}$$

Relation between radius and curvature

$$\Delta\alpha = \underline{\Delta L}/R$$

MINOSC – The **Actuated Catheter**

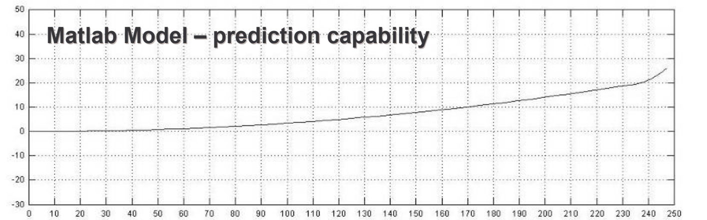

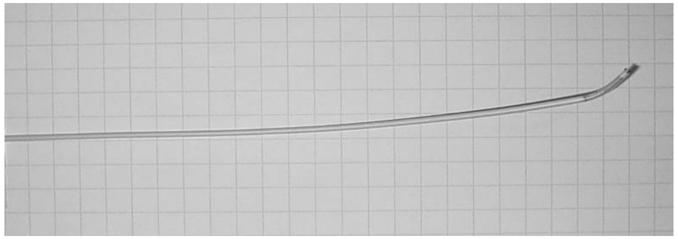

MINOSC – The **Fluidic system**

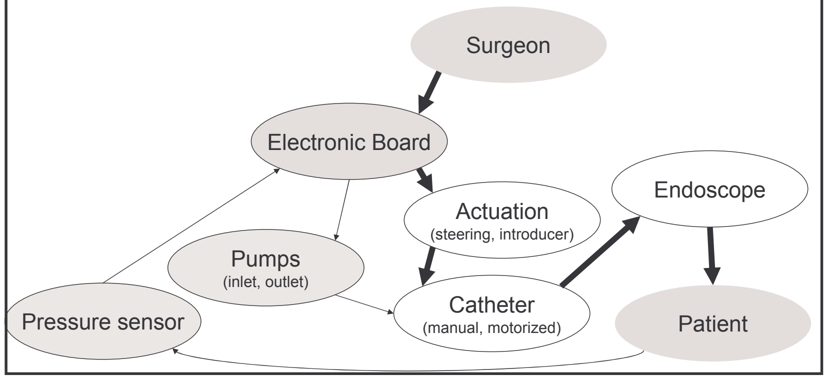

MINOSC – The **Fluidic system**

Fluidic navigation system of a microendoscope exploiting *microjets*, in order **not to touch** the tissue

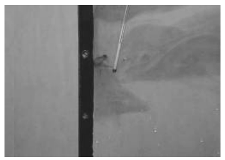

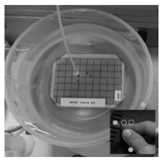

MINOSC – The **Fluidic system**

- The output velocity is the critical parameter (interaction with tissues).
- Driving pressures have therefore to be chosen once safe values for the compression on tissues are imposed.

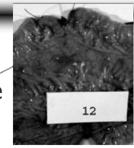

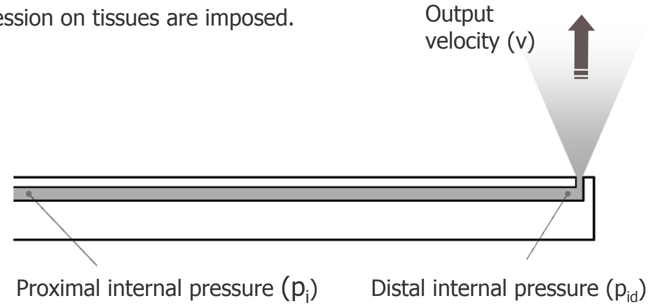

MINOSC – The **Fluidic system**

The kinetics energy of the flow is converted into compression according to the relation (Bernoulli equation):

$$\frac{v^2}{2} = \frac{p}{\rho}$$

"v" is the output velocity,"p" is compression on the tissue, "ρ" is the fluid density

- Localized compressions under 100 grams/cm^2 (0.01 MPa) do not cause any effect on the tissue.
- The maximum allowable velocity is:

$$v = \sqrt{\frac{2p}{\rho}} = 4.4\ m/s$$

MINOSC – The **Fluidic system**

- For an output velocity of 4.4 m/s the proximal pressure to be applied at the catheter is given by the relation (Poiseuille's law):

$$p_i = \frac{8\eta L}{R^2} v = 5.6\ bar$$

"v" is the output velocity,
"L" is the catheter length,
"R" is the duct radius and
"η" is the fluid viscosity

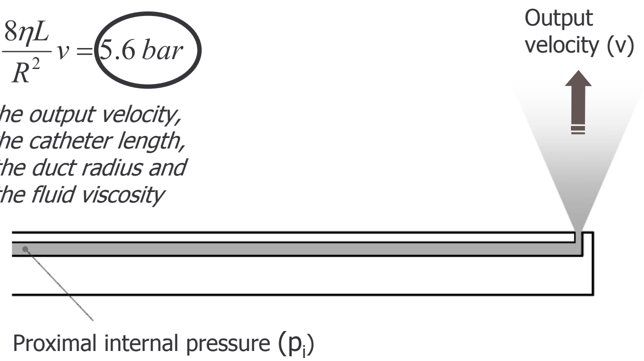

MINOSC – The **Fluidic system**

Valves for flow control

- Proportional valves practically do not exist for small flow control and **high pressures**.
- On/Off valves are availbale in a wide range of performances and at they can be driven at fair high frequency (from tens to hundreds of hertz).

Use of On/Off valves driven in Pulse Width Modulation mode (PWM)

Fluidic Configuration

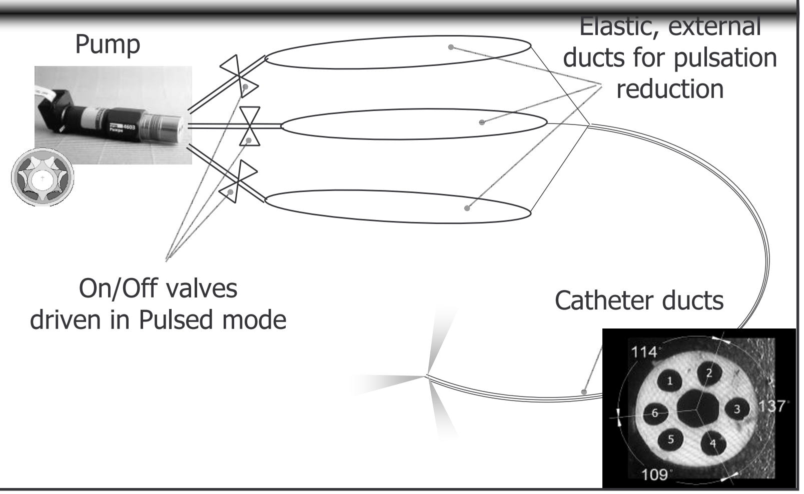

System modelling for PWM driving

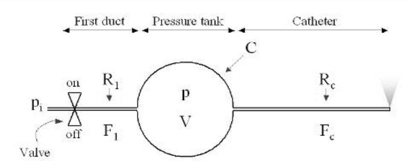

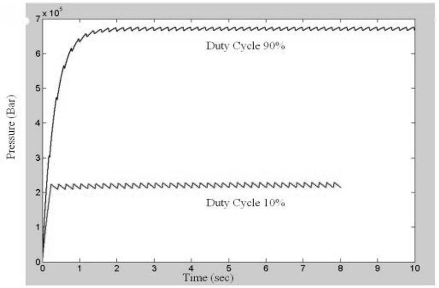

Each of the three jets can be finely tuned thanks to SMALL dimensions, where inertial effects of the fluid are low (10-90 % of full power with low ripple)

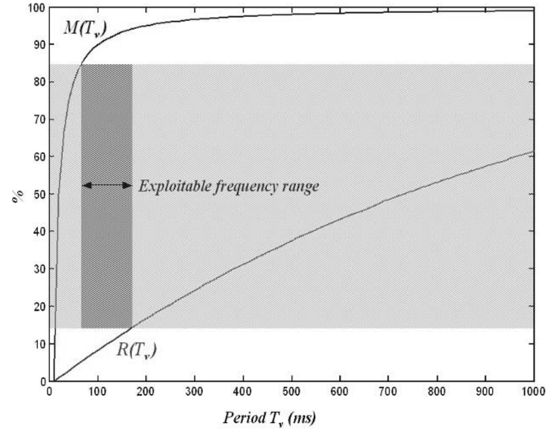

The two parameters to be considered while choosing the working frequency of the valves are **Modulation** (ratio [max. - min.]/max.) and **Ripple**.

Tests

The fluidic steering performances of the catheter have been tested in a water tank provided with a 1mm spaced grid on the bottom. An optic fiber carrying light has been inserted in the central lumen of the catheter, to enable the measuring of the bending action.

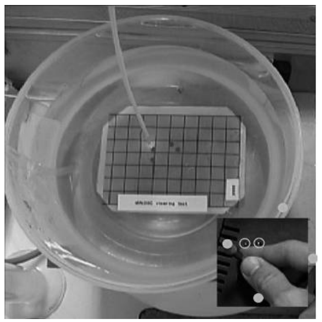

MINOSC – The **Navigation Module**

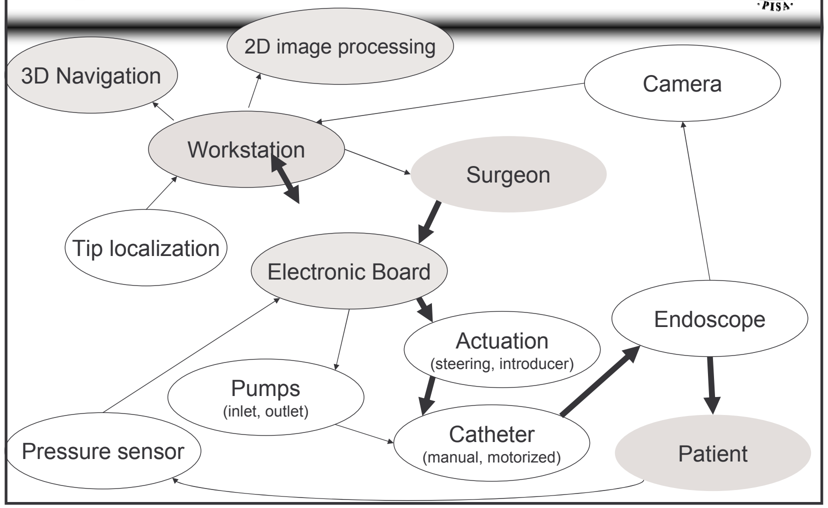

Automatic segmentation of lumen images

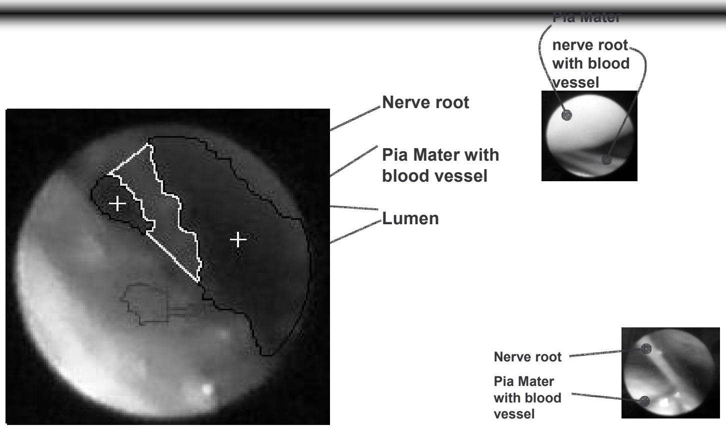

Automatic segmentation of lumen images

1. Adaptive choice of color threshold;
2. Image "binarization";
3. Blobs identification;
4. Filter on their minimal size.

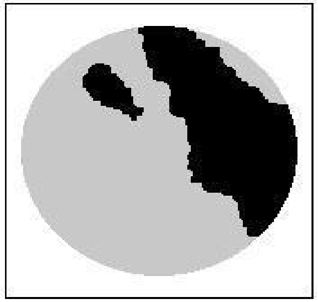

Automatic segmentation of lumen images

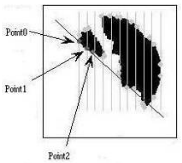

Point2 is left of the oriented line passing through Point0 and Point1. The three Points do not generate any concavity.

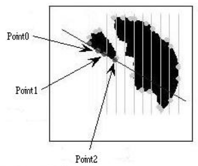

The three points lie on the same line and they do not generate any concavity.

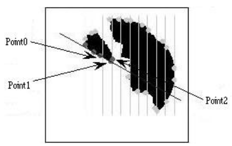

Point0, Point1 and Point2 do not generate any concavity.

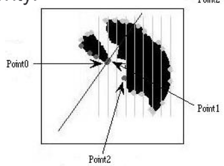

The three points generate a concavity. Such a concavity cannot be generated by a wall. Point1 is deleted.

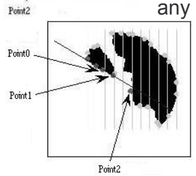

The three points generate a concavity but it can be generated by a wall. Point1 is not deleted.

Some segmented images

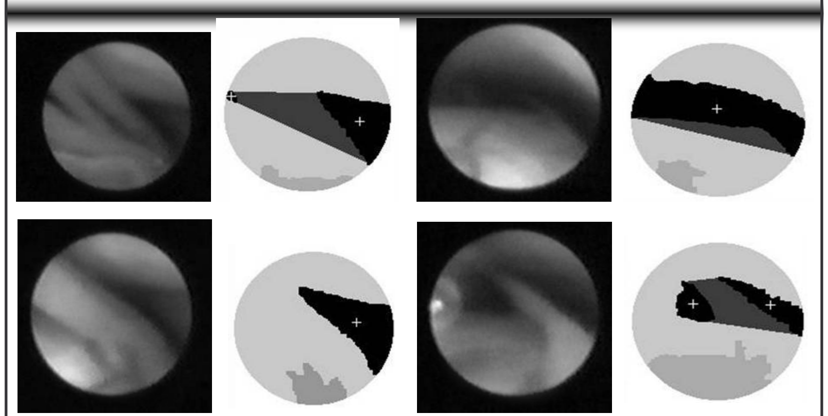

Understanding what's around me

3D Navigation

While advancing, structures like nerve roots and vessels disappear, but remains dangerous to knock against!

"Rear-view mirror" concept

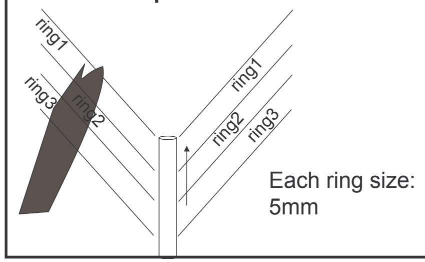

Each ring size: 5mm

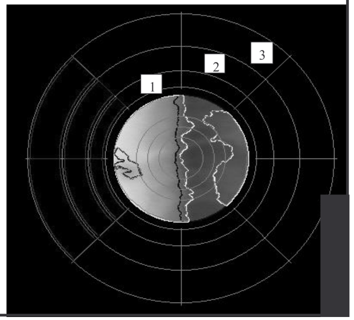

Mock-ups of the spine

Creating "artificial" testbeds for in vitro experimentation and preliminary validation of the MiNOSC endoscope

The Visible Human Female Dataset

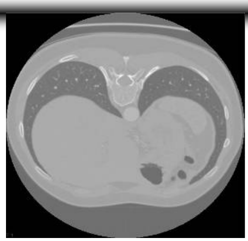

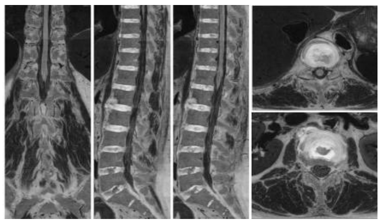

- CT scan: for labeling of bone structures
- Color images: for labeling of arachnoid and spinal cord

Segmentation and labeling

- We used commercial software Analyze 4.0/5.0:
  - Read DICOM format (and many others)
  - Has a lot of tools for automatic, semiautomatic and manual segmentation
  - Export data in an open format
- We segmented:
  - All vertebrae (from CT)
  - Discs (from CT)
  - Arachnoid (from color images)
  - Spinal cord (from color images)

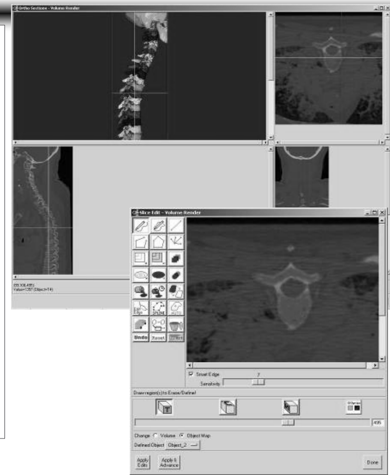

Splitting of labeled volume

- This is needed for fitting the objects inside the 3D printer workspace

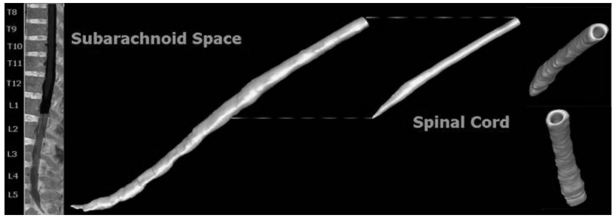

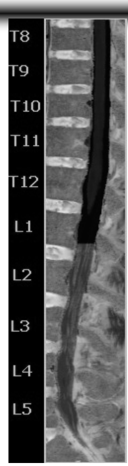

Surface extraction

- We used the Marching Cubes algorithm
- **But** Analyze surface extractor module (based on Marching Cubes) generates surfaces with holes.

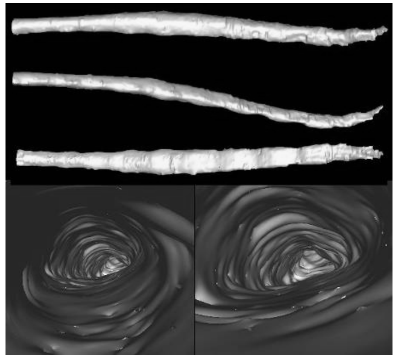

Surface extraction

- Holes in the extracted surfaces introduce errors during the 3D print of the objects.
- We implemented a corrected version of the algorithm generating topologically correct surfaces.
- We used VTK to improve the quality of the extracted surfaces

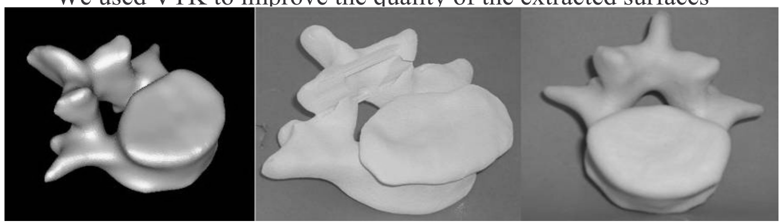

The 3D Model of the bones

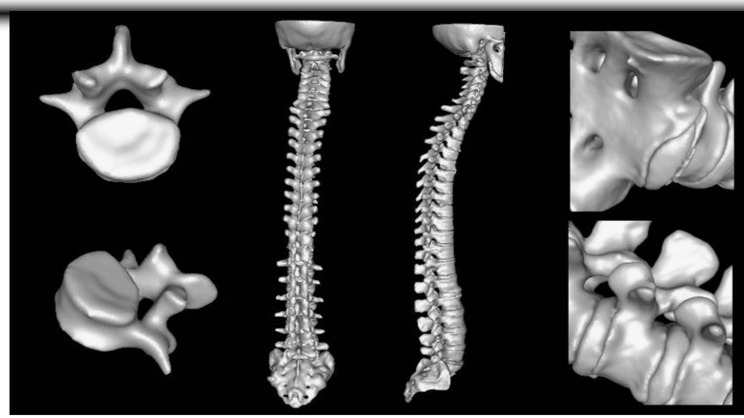

Singol components Assembled Spine Model Details of fitting of the components

The 3D Model of the bones

- Vertebras (rigid material: diretly from 3D printer)

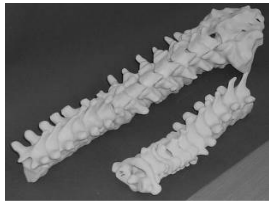

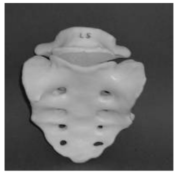

The physical objects

- The arachnoid and the spinal cord (soft material: silicon)

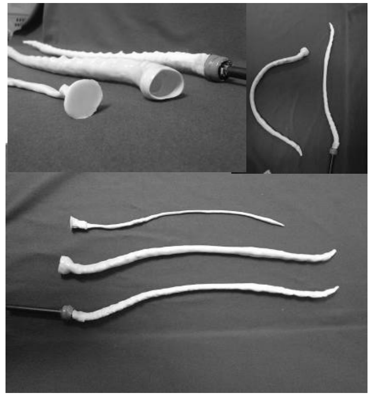

The "real scale" spine model

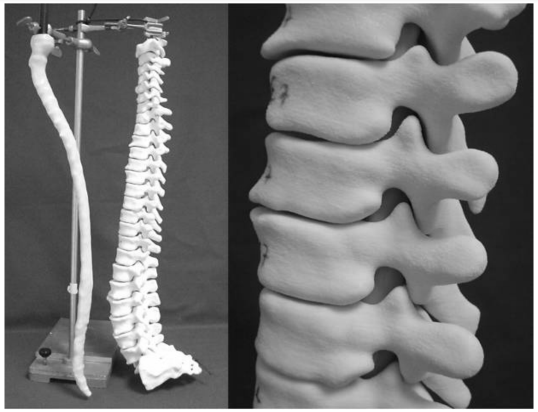

Partially assembled: vertebra + arachnoid

Experimental real time navigation

Real-time anatomy recognition

——	Lumen
——	Nerves
——	Membranes
——	Blood vessels
——	Dirty lumen

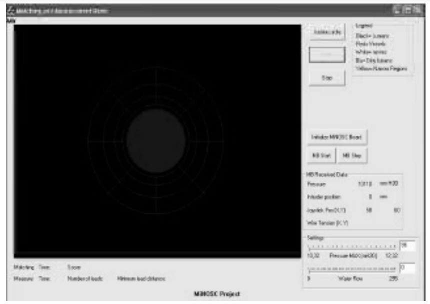

"Rear-view mirror" concept

In-vivo validation

In vivo experiments in pigs in Ozzano (Bologna), 2002-2005.

Successful endoscopy (see images below) of the whole spinal cord, from lumbar access up to cervical tract, with **direct nerve stimulation through endoluminal electrode**

Pia Mater

nerve root with blood vessel

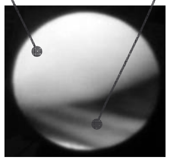

Nerve root

Pia Mater with blood vessel

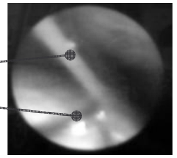

FETAL SURGERY: a field to be opened from the instrumentation view point

Endoscopic access to the fetoplacental unit: from experimental to clinical applications.

Research programme set up by the K.U.Leuven, funded by the European Commission, Biomed II

About the research programme

- WHAT IS FETOSCOPY?
- THE EUROFOETUS PROGRAMME.
- THE EUROFOETUS OBJECTIVES.
- THE FOUNDING RESEARCH GROUP.

About the clinical studies (open to all centers)

- THE INTERNATIONAL FETOSCOPY REGISTRY.
- THE TTTS RANDOMISED TRIAL.
- THE TTTS OBSERVATIONAL STUDY.
- LIST OF PARTICIPATING CENTERS.

Direct links

- REGISTRATION AS A NEW PARTICIPATING CENTER.
- ACCESS TO THE STUDIES.
- THE TTTS RANDOMIZED TRIAL PROTOCOL
- FORMS USED IN THE STUDY

Micro-SURF

Micro Instrumentation for Fetal Surgery

A research project funded by *Cassa di Risparmio di Pisa*

Starting date: 1/1/2005

Project length: 2 years

Partners:

- CRIM Lab – Scuola Superiore Sant'Anna, Pisa, Italy (Coordinator)
  - Prof. Dario
- IFC – CNR Pisa and Massa, Italy
  - Prof. Coceani, Prof. Murzi
- Department of Pediatrics, Faculty of Medicine and Dentistry, Alberta, Canada
  - Dr. Yashu Coe

Clinical Target 1 – Spina Bifida:

Incomplete closure in the spinal column

©Time

©Dr.Bruner Vanderbilt univ.

Large Incision

⇩

Early Delivery

Spina bifida or myelomeningocele is a neural tube defect resulting in incomplete closure within the spinal column, usually found on the lower parts of the fetus back. The exposure of the opened spinal code to amniotic fluid worsens the disabilities of the baby after birth and the disabilities usually include paralysis of the lower limbs, urinary dysfunction and hydrocephalus (brain disorder).

Clinical Target 2 – Pulmonary Atresia:

To distinguish obstructed pulmonary valve from the walls of the heart in fetus during prenatal minimally invasive cardiac surgery

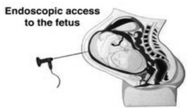

In Pulmonary atresia with intact ventricular septum the pulmonary valve leaflets are completely fused and form a membrane between right ventricle and pulmonary artery

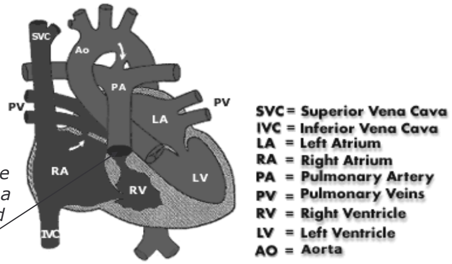

Surgical intervention after birth allows to link up the right ventricle to the pulmonary vein, but the ventricle remains not fully grown, with serious consequences on the individual health during his/her life. To date the most common intervention is therapeutic abortion.

In the field of fetal surgery research, attempts with Radio-Frequency catheters are being performed, with a low rate of success (mainly due to localization problems).

Motivation – Fetal Surgery

Proposed surgical Procedure:

Intrauterine* closure using *MRI compatible robots

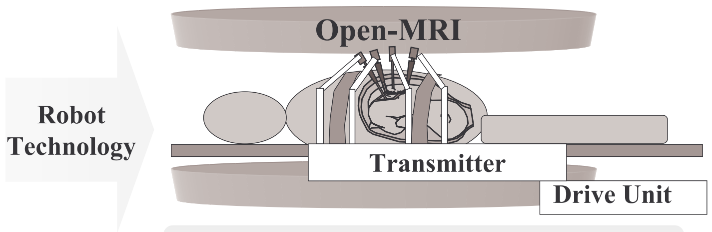

Minimally invasive surgery

Proposed Surgical Procedures

the amount of amniotic fluid is controlled to make surgical space

An endoscope is inserted

Abdominal and uterine walls must be penetrated <u>at the same time</u> not to damage uterine inner membranes

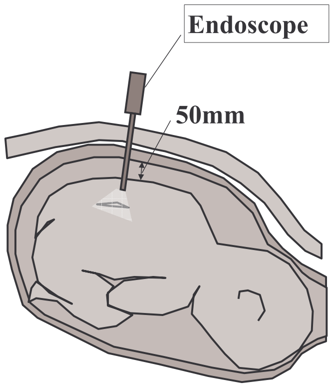

Proposed Surgical Procedures

A stabilizer is inserted

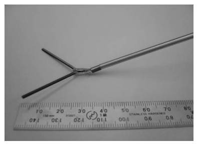

The surgical area is stabilized with <u>suction force</u>

Strong pushing force could result in paralytic lower limbs

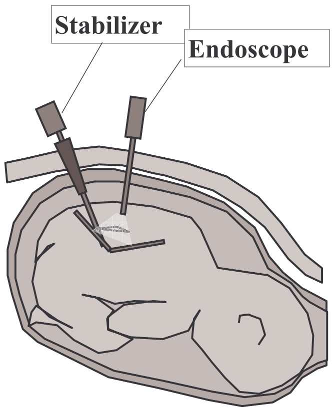

Proposed Surgical Procedures

Two surgical manipulators are inserted so that their tips could cover the surgical area

Move the set-up bed into an Open MRI

Suturing

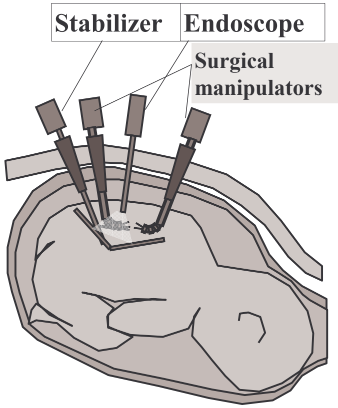

Micro-Surf Main Goal

Design and development of sensorized endoscopic instrumentation for minimal invasive fetal surgery

Sensorized Tools' Objectives

To distinguish the different physiological tissues during surgical intervention, in order to assess exactly the pathological area.

Special Requirements

- High miniaturization;
- Ability to perform tissues identification;
- Integration into commercially available catheter system for MIS;
- Compatibility with special imaging techniques (e.g. Open-MRI).

Work Flow

1. Modeling of involved tissues;
2. Development of sensors' prototypes;
3. Experimental validation;
4. Technology transfer.

Work On Going

A Three Components Force Sensorized Tip for Minimal Invasive Surgery and Catheterism

Overall Dimensions

- Outer diameter: **7 mm**
- Outer diameter foreseen for the next prototype: **2.3 mm**

Components

1. Ruby Knife
2. External Upper Part
3. Acrylic Ball
4. Soft Polyurethane Filling
5. 3 Axial Force MicroSensor
6. External Lower Part

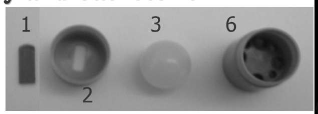

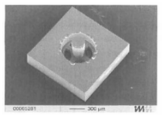

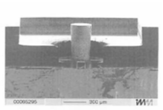

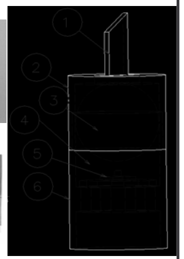

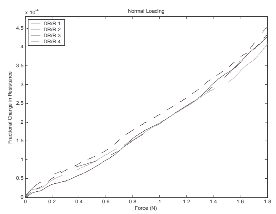

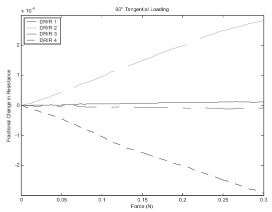

Work On Going

A Mechatronic System for Tissue Palpation and Electrical Impedence Measurement

Overall Dimensions

- Outer diameter: **2.75 mm**

Features

1. Contact force Sensing;
2. Tissues' electrical impedance measurement;
3. One lumen available for surgical instruments.

Objective

- To distinguish among different tissues thanks

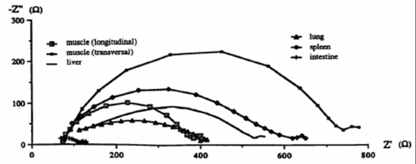

Figure 1 - Impedance loci of tissue samples excised from sheep

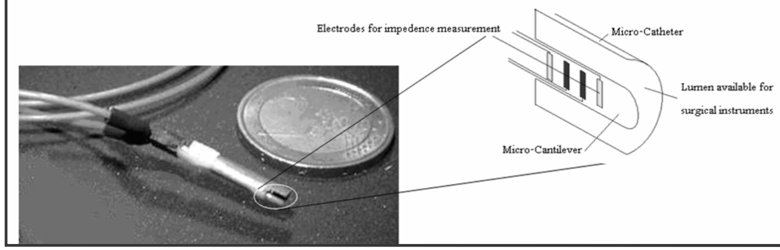

Bio-Mechanical Modeling and Soft Tissue Indentation

Bio-mechanical modeling of myocardial tissue → **Mini-Instron for in-vitro tissue characterization**

Definition of Strain energy function W for myocardium tissue considered as a hyperelastic and anysotropic material

$$\rho W = \frac{c}{2} e^{Q} + P$$

$$Q = a_1 E_1^2 + a_0 E_0^2 \qquad P = \frac{1}{3}\left(b_1 E_1^3 + b_0 E_0^3\right) + \frac{1}{2}\left(d_1 E_1^2 + d_0 E_0^2\right)$$

Solving the inverse problem for bio-mechanical tissue indentation by using Finite Element Analysis

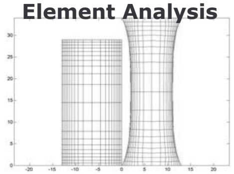

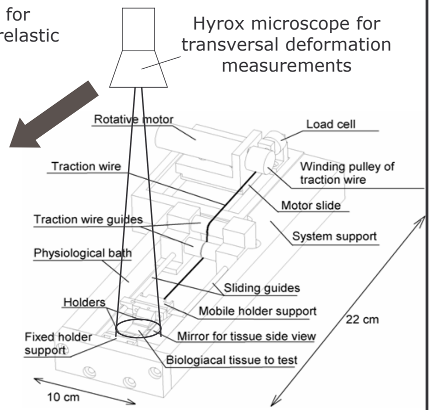

Specifications of the manipulator

<u>Outer diameter</u>

Incision on the uterus must be < 3mm
(when the incision is < 3mm, it closes without suturing)

→**Outer diameter of the cannula < 3mm**

→**<u>Outer diameter of the manipulator</u> < <u>2.6mm</u>**

<u>Dexterity</u>

High dexterity for cutting and suturing in small surgical area

<u>more D.O.F and small bending radius</u>

<u>Material</u>

<u>MRI compatibility</u> is necessary

Micro manipulators (2001)

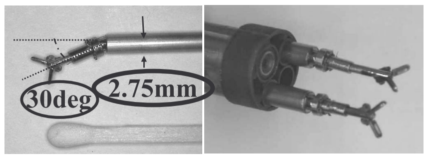

Asemble without a screw

- Diameter
  (less than 2.6mm)
- more dexterity
- MRI compatible

- **O.D：2.75mm→2.4mm**
- **Joint： 1→2**
- **Bending Degree：30 deg→90 deg**
- **SUS →Ti**
- **DC motor →US motor**

Design of bending mechanism

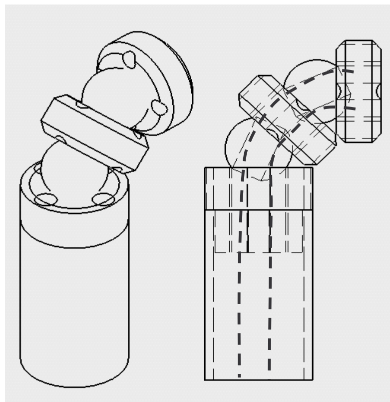

<u>The features of the mechanism</u>

- **small diameter(2.4mm)**
- **small bending radius(2.45mm)**
- **ease of fabrication (low cost)**
- **high rigidity**
- **applicability for other surgical applications**

Fabricated parts

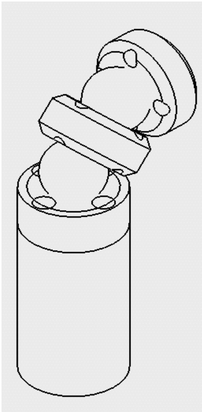

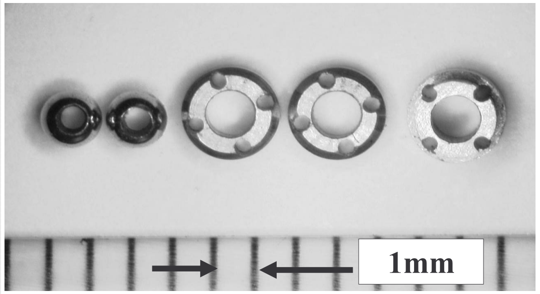

Fabricated by traditional machines

Tip of surgical manipulator

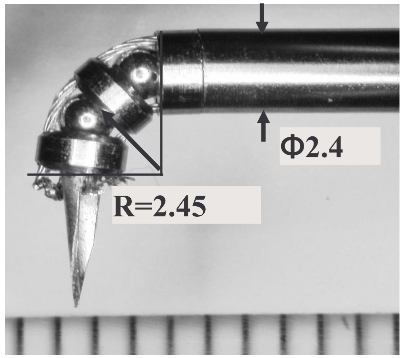

Rigid

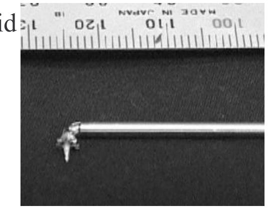

Flexible

Collaboration between Waseda University and CRIM Lab.

Research at Prof.Higuchi Lab

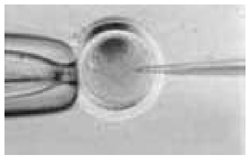

Pulse insertion driven with a PZT actuator is good for soft tissue

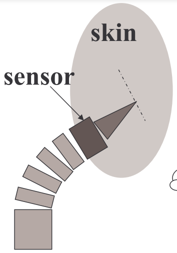

Intentional Vibration for achieving sharp cutting

With MEMS force sensor…

- **Precise position of the knife**
- **Force on the knife**

State of the art in surgical sensors

Data knife – Verimetra Inc.

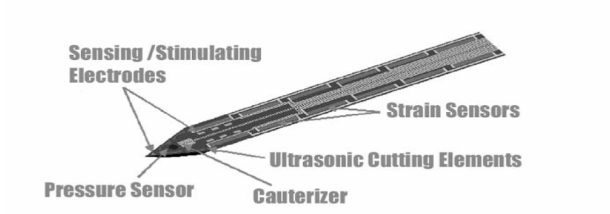

- Electrodes to classify tissues (impedance measurement)
- Pressure sensor to identify materials surrounding the scalpel
- strain gauge sensor to measure the applied force

State of the art in surgical sensors

Sensorized Scalpel

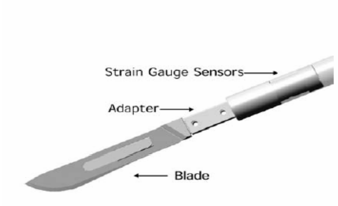

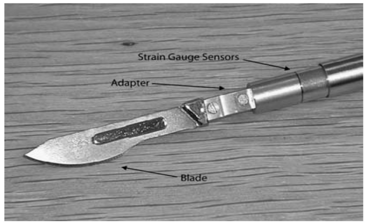

- Force measurement in all directions (4 channels, 3x force and 1 x torque)
- Force can be measured up to 20 N
- diameter: 10 mm
- designed for MIS

T J Ortmaier, "Motion Compensation in Minimally Invasive Robotic Surgery", Technical University of Munich, 2003, pp 15-16

State of the art in surgical sensors

Sensorized Catheter Tip

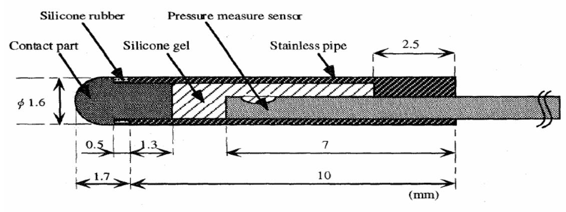

Micro force sensor for intravascular neurosurgery and in vivo intervention
1 Component Force Sensor for detecting frontal pushing force

M. Tanimoto, F. Arai, T.Fukuda, H. Iwata, K. Itoigawa, Y. Gotoh, M. Hashimoto, M. Negoro, Micro, „Micro force sensor for intravascular neurosurgery and in vivo experiment", in Proc. IEEE International Workshop on Microelectromechanical Systems (MEMS `98), Heidelberg, Germanym Jan. 1998, pp. 504-509

State of the art in surgical sensors

Sensorized Catheter Tip - Olympus

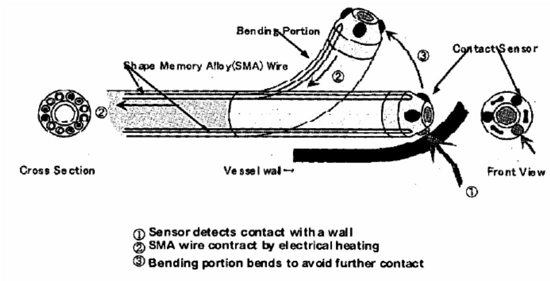

3 semiconductor strain gauges (contact sensors) are placed at the head at 120° intervals each facing one of the three SMA wires for closed loop control

Our sensorized tip
Design of the first prototype (7.4 mm)

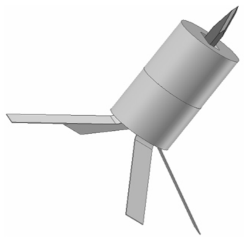

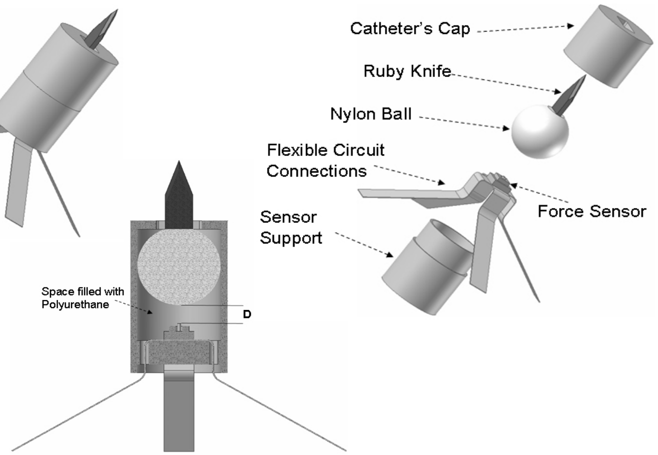

Assembly Process

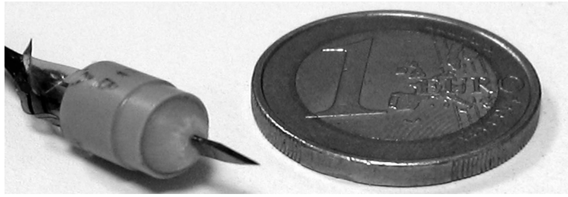

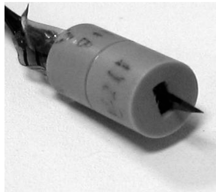

3 Components Force MicroSensor

1.5mm x 1.5mm silicon 3 axial microsensor

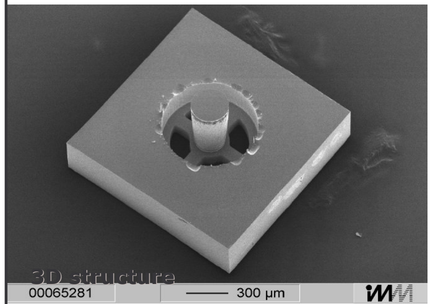

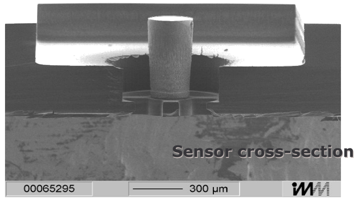

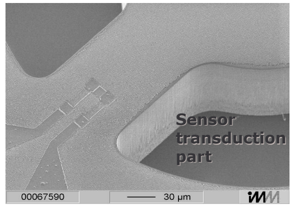

L. Beccai, S. Roccella, A. Arena, F. Valvo, P. Valdastri, A. Menciassi, M. C. Carrozza, P. Dario, "*Design and fabrication of a hybrid silicon three-axial force sensor for biomechanical applications*", Sensors and Actuators A, Vol. 120, No. 2, pp. 370-382.

Micro Sensor output signals

- 4 Output Signals
  - One fractional change in resistance ΔR/R per piezo resistor
  - Transduction to voltage signals by 4 Wheatstone bridge amplification channels

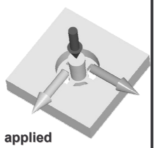

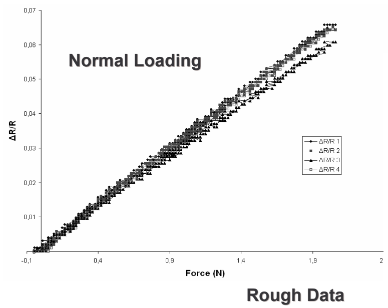

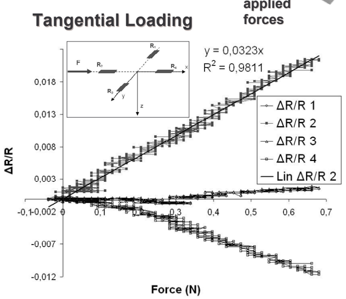

Micro Sensor output signals

- Once the vector of the four ΔR/R is acquired, it has to be converted in a 3 components (F_x, F_y and F_z) force vector by:
- The calibration matrix K can be evaluated by a previous sensor characterization [see Ref]. A typical K matrix is:

$$F = K\,\frac{\Delta R}{R}$$

$$K = \begin{pmatrix} 0 & 5.3 & 0 & -4.6 \\ -4.9 & 0 & 4.86 & 0 \\ 6.65 & 5.62 & 4.73 & 5.89 \end{pmatrix} N$$

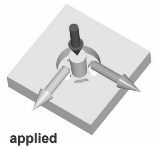

3 Axial Force MicroSensor: Example of Packaging and Signal Processing

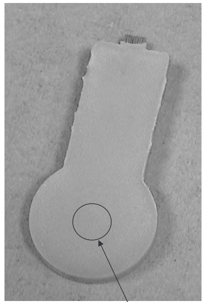

Embedding of the 3 Axial Micro Force Sensor in a Soft Polyurethane Matrix

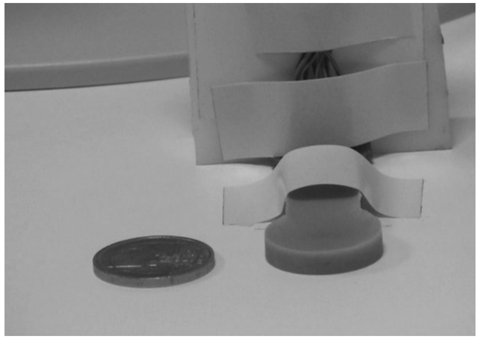

Typical output from the 3 axial force microsensor using the calibration matrix
- The 3 components of the force are transduced by the sensor and plotted on a 3D surface

Experimental SetUp

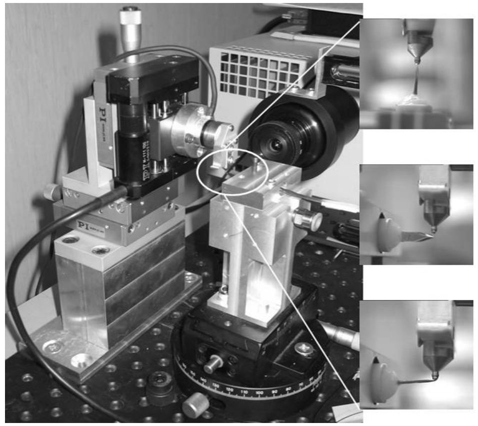

Results: Normal Loading (Z axis)

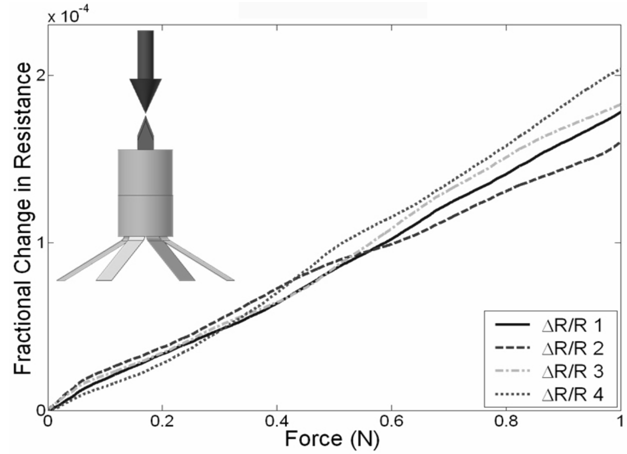

Results: Tangential Loading (X axis)

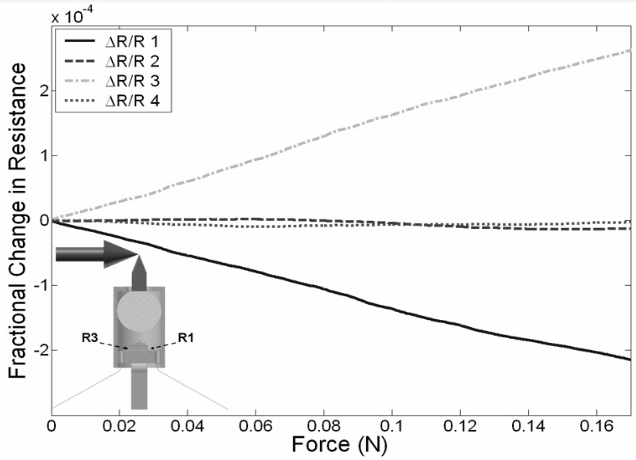

Results: Tangential Loading (Y axis)

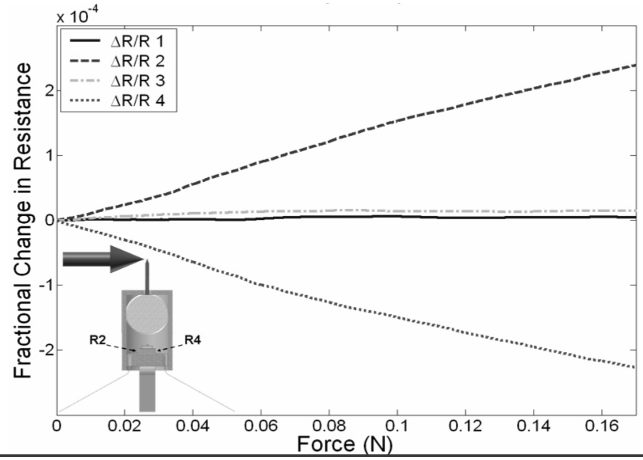

CRIM Platform Components

Through PC-Link:
Movement Control

- Haptic Device
  - 6 d.o.f. in sensing
  - 3 d.o.f. in force feedback

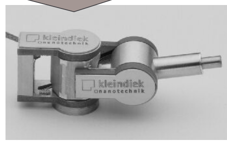

- Nanomanipulator
  - 3 d.o.f. in movement
  - Nanometric Step Resolution

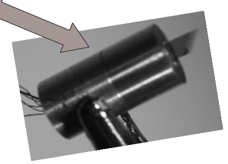

- Sensorized Catheter
  - Placed on the nanomanipulator tip
  - Embedding a 3 axial force microsensor

Through 3 axial force sensor:
3D Force Feedback

Haptic Device

Phantom 1.5

Workspace	7.5 x 10.5 x 15 inches 19.5 x 27x 37.5
Range of Motion	Lower arm movement pivoting at elbow
Nominal position resolution	860 dpi 0.03 mm
Backdrive friction	0.15 oz. 0.04 N
Maximum exertable force	1.9 lbf. 8.5 N
Continuous exertable force (24 hrs)	0.3 lbf 1.4 N
Stiffness	20 lbs./in. 3.5 N/mm
Inertia (apparent mass at tip). Without Encoder Gimbal	< 0.17lbm. < 75 g
Footprint	10 x 13 inches 25 x 33 cm
Force feedback	x, y, z
Position sensing	x, y, z (6DOF optional)
Interface	Parallel Port
Supported platforms	Intel-based PCs

Nanomanipulator

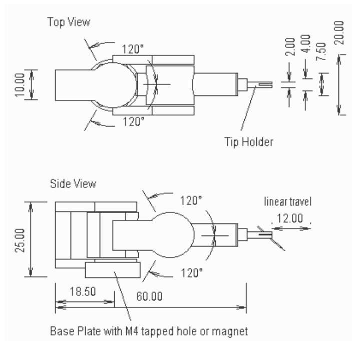

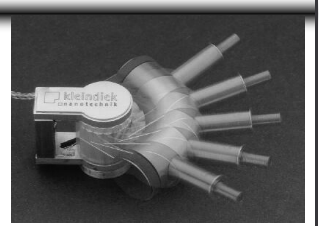

- Sub nanometer precision, "Nanomanipulator".
- More than 100 cubic centimeter working range.
- Piezoelectric actuation.
- Extremely robust and compact construction.
- UHV compatible.
- Works at low temperatures.
- Easy mounting with magnetic foot or M4 screw.
- Intuitive control with joysticks or handwheels.

Remarks on the system

The sensor can detect…

- **Force on the knife**
- **Direction of the force on the knife**

The position and force on the knife are calculated using this sensorized catheter without clear view

Future Work

- **Realization of a smaller prototype (outer diam around 2mm)**
- **Adaptation to specific aplications (i.e. nanomanipulators setup, Minimal Invasive Surgery tools……)**

Sensory feedback for bio-micromanipulation tasks

Research fields: **Tissue Characterization** and many other medical research sectors (e.g. semi-autonomous locomotion systems for colonoscopy, integrated devices for endoscopic exploration of the spinal cord, multifunctional microprobes for the detection of key parameters of organ viability for transplantation)

Applications:

- Tissue **diagnosis** in medical screening
- Tissue **recognition** and identification in Minimally Invasive Surgery
- Tissue **modeling** for Computer Assisted Surgery
- Development of tissue-tailored surgical tools

Key points:

- Smart miniaturized instruments with tactile feedback for operating in difficult situations and delicate small environments
- Flexibility of the system, in order to allow different research lines to be followed

Design issues

Standard requirements for the design and fabrication of purposely developed biomedical microdevices for "*in-vitro*" and "*in-vivo*" applications:

- **Mechanical robustness**
- **Proper electrical insulation**
- **Packaging bio-compatibility**
- **Portability of the tools (to avoid tissue decay)**
- **Possibility of having disposable tools**

Scheme of the CRIM Workstation

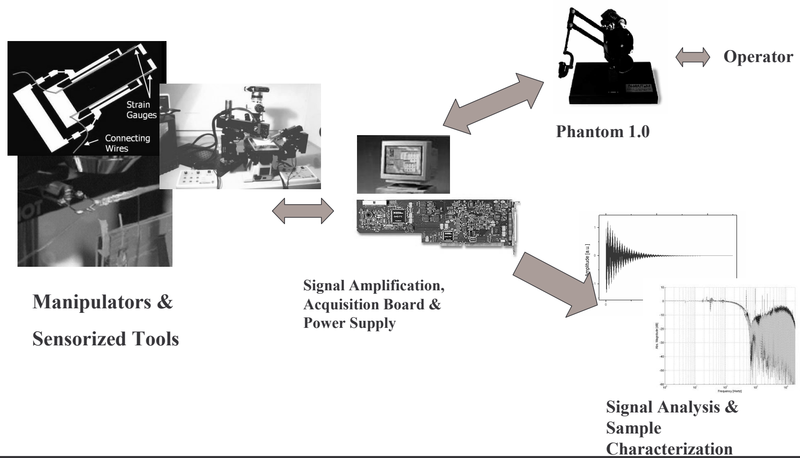

Measurement of mechanical properties of bio-tissues microsamples

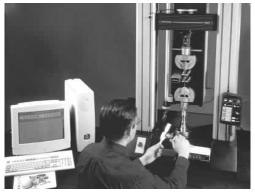

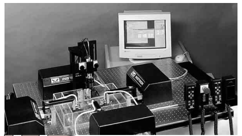

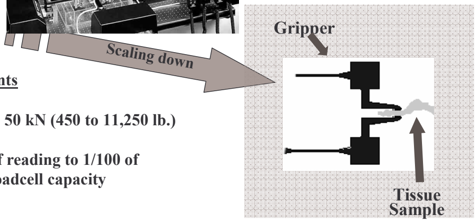

Tensile Test Characterization Instruments

Table-top models (1.5 m X 1 m) for 2 to 50 kN (450 to 11,250 lb.) capacities.
Force measurement accuracy of 0.4% of reading to 1/100 of loadcell capacity and 0.5% to 1/250 of loadcell capacity

In biomedical applications:
Characterization of bones, soft tissues testing etc.

Biomechanical Characterization

Biological tissues as "multifunctional" materials

Biological tissues can be considered as a composite material whose components accomplish one or more functions. Due to the complexity of the whole tissue behavior, that functions have different natures: "mechanical", "chemical", "electrical". Thus, biological tissues are multifunctional materials.

1.muscle
2. muscle fibers
3. single fiber
4. myofibril
5. sarcomere
6. actin filament
7. myosin filament

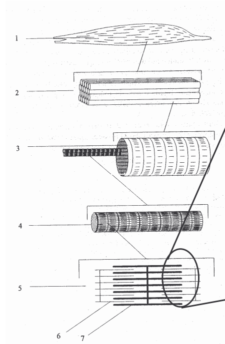

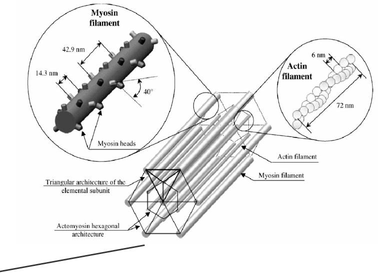

A. Redaelli, M. Soncini, F.M. Montevecchi, "*Myosin cross-bridge mechanics:geometrical determinants for continuous sliding*", Journal of Biomechanics Vol: 34 (2001), pp.1607 –1617

Biomechanical Characterization

"From discrete to continuous" approach$_{1/2}$

The biomechanical characterization of biological tissues has to be related to single discrete components and to their mutual interconnections. Different kind of nano – manipulators (AFM, microneedle, magnetic field, flow field, photonic field) have been used to measure the mechanical characteristics of tissue molecules.

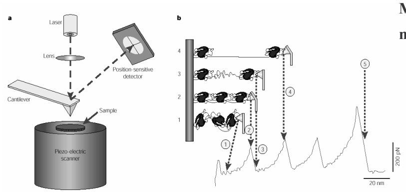

AFM system as test bench for discrete nano-biocomponents

Myosin – Actin filaments force interaction measured by microneedle tip

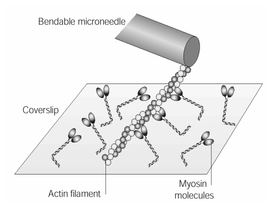

C. Bustamante, C. Macosko, J.L. Wuite, "*Grabbing the cat by the tail: manipulating molecules one by one*", Nature Reviews Molecular Cell Biology (2000), Vol. 1, pp. 130-136

Biomechanical Characterization

"From discrete to continuous" approach$_{2/2}$

To infer continuous constitutive laws from qualitative information (diagram 1 and 2) of discrete elements (e.g. elastin and collagen) an homogenization modeling has to be applied. The homogenization model is a statistic tool which allows to adding, in a statistical way, the mechanical contribution of each element by weighting its orientation and mutual interconnections.

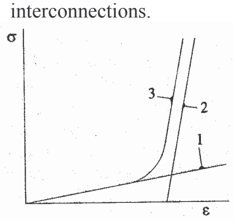

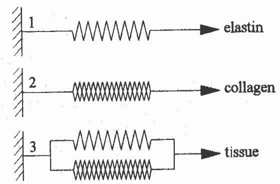

Finally, experimental tests involving the whole tissue can be performed, and their quantitative results (see diagram 3), obtained by solving the mechanical inverse problem, can be used as an useful feedback for the constitutive modeling.

On the right, the experimental configuration of discrete elements (1-2) and whole tissue (3); on the left, the corresponding qualitative diagrams.

Microtools as test micro-machines

Biological tissues have, generally, mechanical properties changing with high gradients in small areas

Local measurement capabilities ensured by microtools are a crucial enhancement compared to those provided by traditional machines

Impulsive or stepping analysis carried out by using microtools allows to extract the dynamic behavior of the material for the whole frequency spectrum by performing a single test instead of the long-drawn-out swapping procedure

This time-reducing procedure is helpful for **avoiding tissue decay**

Modelling approach for in-vitro Tissues Characterization

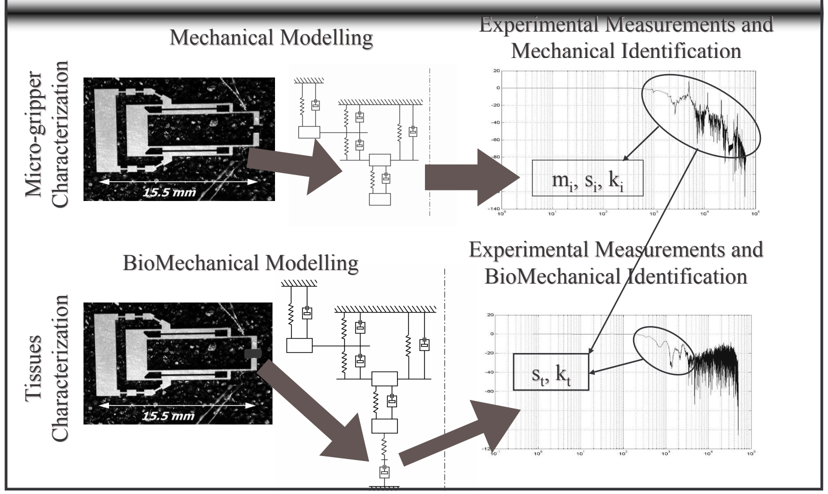

Applications: our experience

- A few examples of our tools, with characterization, applications and experimental tests:
  - LIGA fabricated grippers
  - LASER and EDM fabricated grippers
  - SDM fabricated Smart Catheters

The LIGA Microgripper

LIGA-fabricated Microgripper equipped with four active strain-gauges in a Wheatstone bridge configuration

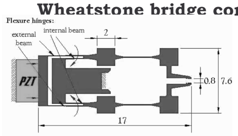

Gripper Dimensions:
Length: 17 mm
Width: 7.6 mm
Thickness : 0.4 mm
Mechanical amplification: 11

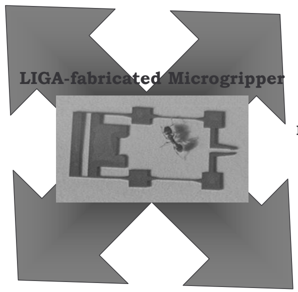

Tokin AE0203D16 :
Max V: 150 V Max displ.: ~ 18 μm
Lenght: 20 mm Cross sect.: 2 x 3 mm²

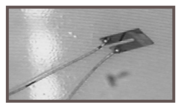

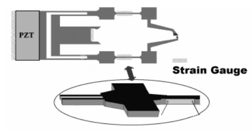

Semiconductor Strain-Gauge (Entran):
- **Electrical resistance: 1,5 KΩ**
- **Gauge factor: 150**
- **Overall dimensions: 1.3 mm x 0.4 mm**

Strain-Gauge Position:
- **Decoupling between actuation and grasping**
- **No sensor output without contact**

The EDM Microgripper

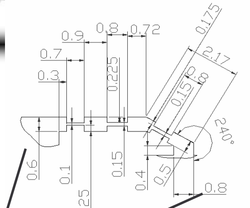

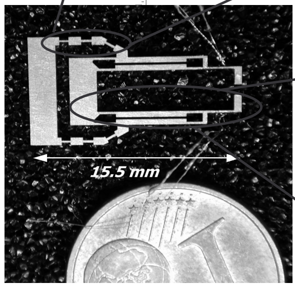

Max span: 2.5 mm (800 μm)
Overall dimensions: 15.5 × 8.4 × 0.5 mm³
Thickness: 0.5 mm
Thinnest beam width: 100 μm
Thinnest beam length: 700 μm
Mass: 160 mg
Work: 5.9*10^{-2} mJoule
Mechanical amplification factor: 4

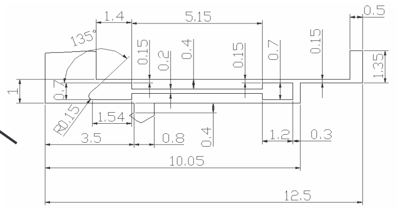

Microgripper Characterization: Experimental Set-up

Microgripper piezoactuated with a large displacement-low voltage actuator

CEDRAT APA100S:

Max V: 150 V **Max displ.: ~ 100 μm**
Lenght: 25 mm **Height × Width: 10 × 9 mm²**

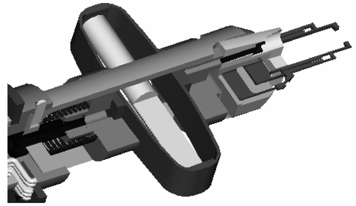

Displacement characterization: laser gauge

Force characterization: load cell

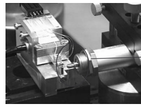

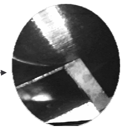

Localization of pulsating microvessels

To restore finger palpation capabilities exploited in traditional "open-field" surgery (characterization of tissue hardness and detection of pulsating vessels) but substantially reduced in MIS.

Open field surgery

Characteristic Force: 0.5 ÷ 5 N
Dimensional Range: 1 ÷ 20 cm

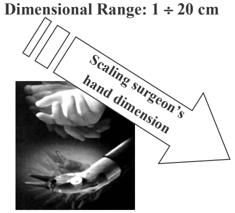

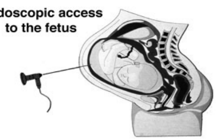

Endoscopic access to the fetus

Prenatal Surgery

Characteristic Force: 50 ÷ 5000 mN
Dimensional Range: 0.5 ÷ 30 mm

State of the art

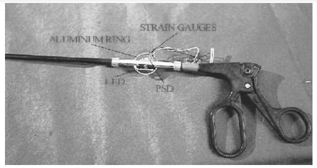

Sensorised laparoscopic tool
(Bicchi et al. - Italy, 1996)

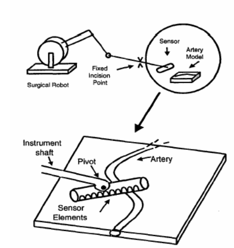

Tactile tracking of arteries
(Beasley et al. - USA, 2002)

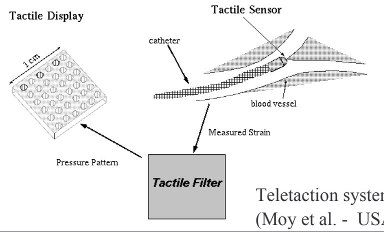

Teletaction system
(Moy et al. - USA, 2000)

Pulsating Microvessels: Experimental Set-Up

Polymeric Microtube (Zeus Scientific Inc) with flowing water pumped by R-NMP Micro-pump

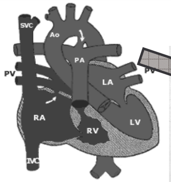

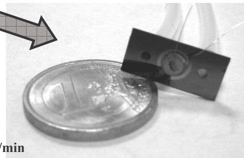

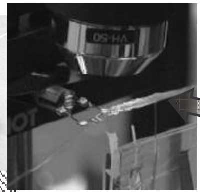

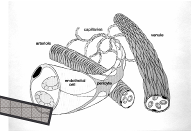

Pumping flow rate = 600 ml/min

Impulsate Modality Frequency = 1÷2 Hz

Ø $_{Ext}$ = 800 µm

Ø $_{Int}$ = 500 µm

Phantom 1.0 Haptic Interface

• Force loop closed by the operator: qualitative user-feedback

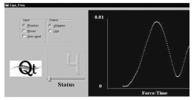

Graphical Interface (Qt)

• Graphical window for sensor output

•Quantitative user feed-back

Force sensing microinstrument for measuring tissue properties and pulse in microsurgery

Menciassi, A.; Eisinberg, A.; Carrozza, M.C.; Dario, P.; IEEE/ASME Transactions on Mechatronics, 2003

Pulsating Microvessels: Experimental Tests

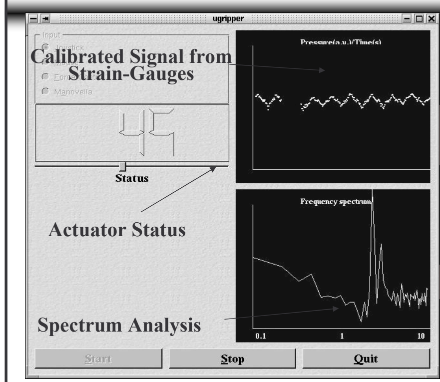

DP=3 mbar

n=3 Hz

At first order the tube can be treated as elastic and so the change of pressure DP is linear with the change of radius DR

From Strain-Gauge signal reading it is possible to obtain frequency and differential pressure values displayed on the graphic interface of the station.

For the Microvessel application required bandwith is extremely low: upper limit of 10-15 Hz (600-900 beats/minute) is sufficient.

Frequency spectrum window is updated every six seconds.

Locating embedded vessels: a furtherly miniaturized tool

Commercial U-shaped polysilicon strain gauge sensors, connected to an external Wheatstone bridge electronic circuit, were embedded into a polyurethane matrix with a desired shape (B) and then in a commercial double lumen catheter (A)

Semiconductor Strain-Gauge (Entran):
• Electrical resistance: 1,5 KW
• Gauge factor: 150
• Overall dimensions: 1.3 mm x 0.4 mm

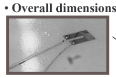

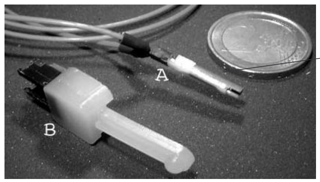

(A) SDM sensorized catheter
(B) “Macro” SDM end-effector

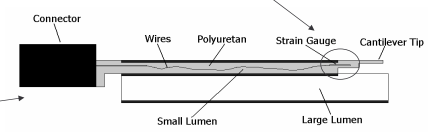

Schematic drawing of the SDM sensorized catheter

The catheter is equipped by an asymmetric double lumen (Φ 2.75 mm). The connecting wires of the strain gauge sensor are placed in the smaller lumen (0.6 mm in height); the big one can be used for the data transmission of different signals (e.g. optic fibre for vision tasks, radio frequency for ablation tasks).

"A teleoperated SDM-based microinstrument for vessel recognition during MIS”

A. Eisinberg, I.Izzo, P.Valdastri, A.Menciassi and P.Dario, MechRob’04

Simulators for embedded vessels

- Soft small tubes (**Ø** $_{\textbf{Ext}}$: 3 mm; **Ø** $_{\textbf{In}}$: 1.5 mm) were employed as vessels simulators.
- The tubes were embedded in a two-component silicon polymer to functionally substitute the biological tissue.
- Two shapes have been selected, in order to test the system capabilities in different modalities.

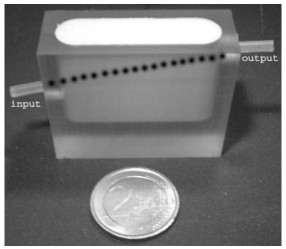

Simulator 1: To distinguish different depths of an embedded pulsating vessel

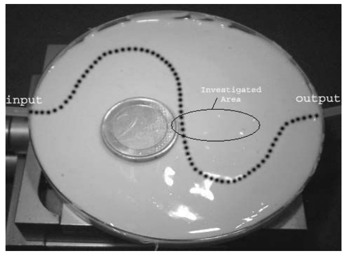

Simulator 2: To measure the end–effector tracking ability, that is to locate the vessel inside tissue at the same depth

The experimental set-up

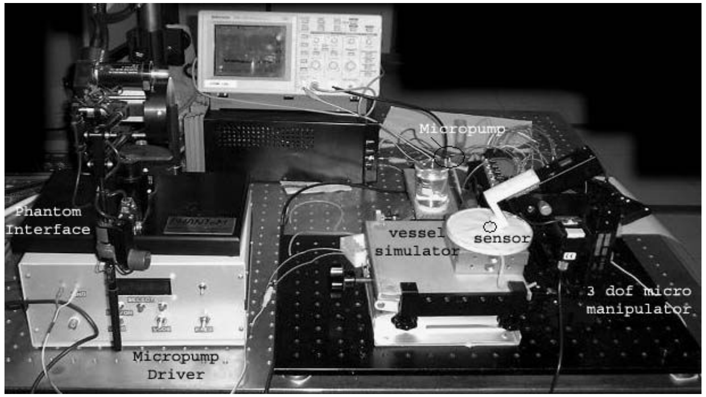

Experimental tests (1/2)

Six unskilled operators were asked to perform the task according to the following procedure:

- **Phase 1**: the problem is briefly illustrated to the operator;
- **Phase 2**: the operator puts the end-effector in position onto the simulator;
- **Phase 3**: the operator feels the force feedback by means of the Phantom haptic interface;
- **Phase 4**: the operator changes the end-effector position and restarts from phase 2 for 4 different positions.

All the operators successfully performed both the recognition and the tracking tasks and stated that the developed system is user friendly.

Experimental tests (2/2)

After a post–processing of the sensor signal, required because of the absence of the thermal compensation and of its high frequency noise, the following results were obtained:

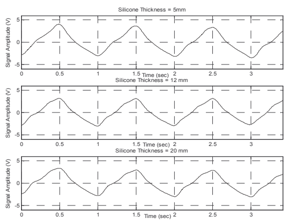

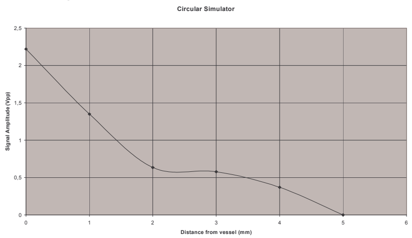

Simulator 1:
Sensor output signal at different vessel depths (the signal frequency is 1 Hz, as the working frequency of the micropump)

Simulator 2:
Signal output amplitude vs. distance from the embedded vessel simulator.
Starting from immediately above the vessel and moving away from it, the decreasing of the signal output amplitude was observed

Development of a Tethered Epicardial Crawler for Minimally Invasive Cardiac Therapies (Patronick, Zenati, Riviere, 2004)

Main Features:

Beating-heart cardiac therapies that can be performed within the pericardium;

Device equipped with the ability to adhere to the surface of the epicardium and locomote to any position and orientation under the direct control of a physician;

It obviates cardiac stabilization, lung deflation, differential lung ventilation, and reinsertion of laparoscopic tools.

These advantages will result in greater efficiency and reduced trauma for the administration of intrapericardial therapies.

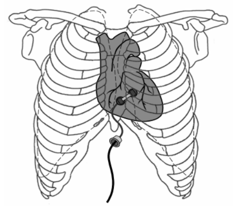

http://www.cs.cmu.edu/~heartlander/index.html

Heart Surgery in Brescia, Italy

Prof. Claudio Muneretto, Gianluigi Bisleri, Aldo Manzato

- Dec 23, 2003: First closed-chest intervention in Europe for treatment of atrial fibrillation.
- Jan 19, 2004: First worldwide intervention of multiple aorto-coronary artery bypass grafting **in the awake patient without general anesthesia.**
- Feb 17, 2004: First worldwide intervention of open-heart cardiac valve substitution **in the awake patient**.
- Jun 24, 2005: First closed-chest worldwide intervention for treatment of atrial fibrillation **in the awake patient**.

The future of heart surgery

The use of minimally invasive techniques **without general anesthesia** allows treatments that are less traumatic, less painful, and less expensive. Our aim is to carry out **most heart surgeries with closed chest**

Prof. Claudio Muneretto
Cattedra di Cardiochirurgia dell'Università di Brescia
Spedali Civili di Brescia